Radiation Measurements 56 (2013) 111–115

Contents lists available at SciVerse ScienceDirect

Radiation Measurements

journal homepage: www.elsevier.com/locate/radmeas

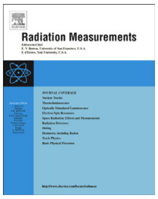

Evaluation of Ce^{3+} and alkali metal ions Co-doped $LiSrAlF_6$ crystalline scintillators

Shingo Wakahara [a,*], Takayuki Yanagida [b], Yutaka Fujimoto [a], Yuui Yokota [a], Jan Pejchal [a,c], Shunsuke Kurosawa [a], Shotaro Suzuki [a], Noriaki Kawaguchi [a,d], Kentaro Fukuda [d], Akira Yoshikawa [a,e]

[a] Institute for Materials Research, Tohoku University, 2-1-1 Katahira, Aoba-ku, Sendai, Miyagi 980-8577, Japan
[b] Kyushu Institute of Technology, Hibikino 2-4, Wakamatsu-ku, Kitakyushu, Fukuoka 808-0196, Japan
[c] Institute of Physics, Academy of Sciences of The Czech Republic, Cukrovarnicka 10, 162 00 Prague 6, Czech Republic
[d] Tokuyama, Co. Ltd., Shibuya 3-chome, Shibuya-ku, Tokyo 150-8383, Japan
[e] New Industry Creation Hatchery Center (NICHe), 6-6-10 Aoba, Aramaki, Aoba-ku, Sendai, Miyagi 980-8579, Japan

HIGHLIGHTS

- ► Ce-doped and alkali metal co-doped LiSAF crystals were grown by μ-PD method.
- ► Alkali metal co-doped crystals showed higher light yield than Ce only doped crystal.
- ► Decay time of alkali metal co-doped LiSAF were longer than that of Ce only doped one.

ARTICLE INFO

Article history:
Received 16 October 2012
Received in revised form
5 December 2012
Accepted 18 December 2012

Keywords:
$LiSrAlF_6$
Thermal neutron
Ce^{3+} 5d-4f transition

ABSTRACT

High scintillation efficiency of Eu-doped $LiSrAlF_6$ (LiSAF) and $LiCaAlF_6$ (LiCAF) codoped with alkali metal ions has been reported in our recent studies. Thus in this paper, we demonstrated the scintillation properties of 1% Ce-doped LiSAF crystals with 1% alkali metal ions co-doping to increase the light yield and understand the scintillation mechanism. The crystals showed intense emission band corresponding to the 5d-4f transition of Ce^{3+}, and their light yields under thermal neutron excitation were higher than that of the Ce only doped crystal. Especially, the light yield of Ce–Na co-doped crystal exceeded about two times that of Ce only doped one.

1. Introduction

Recently, the study of the alternative thermal neutron detection techniques have been started because the supplies of ^3He gas have been diminished due to its increased demand in the world (Kouzes et al., 2010). The techniques are used in a wide variety fields such as homeland security, astrophysics, oil well logging and so on. In the search for new scintillators, various scintillation properties are generally required, for example, high light yield, fast response, low hygroscopicity and linearity of the scintillation response with respect to the incident radiation energy. In the case of thermal neutron scintillator, the large capture cross-section for thermal neutron is important parameter for the host scintillator matrix. Therefore, we have studied ^6Li-containing inorganic crystal as the host material because ^6Li isotope may capture thermal neutrons and convert them into ionizing particles according to the reaction (1).

$$n + {}^6Li \rightarrow {}^3H(2.75\ MeV) + \alpha(2.05\ MeV) \tag{1}$$

The two charged particles produced in the reaction have a total kinetic energy of 4.8 MeV and scintillation light is produced along their ionization tracks. Additionally, low effective atomic number (Z_{eff}) and low density (ρ) are desired to decrease the sensitivity to γ-ray background.

Unfortunately previously developed scintillation materials still have not met all the above requirements, thus our group developed Eu- and Ce-doped LiCAF (Yanagida et al., 2011a; Yokota et al., 2011) and LiSAF (Yamaji et al., 2011, 2012; Yanagida et al., 2011b)

---

* Corresponding author. Tel.: +81 22 215 2214; fax: +81 22 215 2215.
E-mail address: wakahara@imr.tohoku.ac.jp (S. Wakahara).

1350-4487/$ – see front matter © 2013 Elsevier Ltd. All rights reserved.
http://dx.doi.org/10.1016/j.radmeas.2012.12.022

crystalline scintillators. They showed good scintillation performance and no hygroscopicity. Moreover, in recent study, we succeeded to improve the light yield by co-doping with alkali metal ions, especially, the Na co-doped Eu:LiCAF outperformed the Eu:LiCAF by about 30% with its light yield of 40,000 ± 4000 ph/n (Yanagida et al., 2011c). In the case of the Ce doped ones, though they showed fast response assigned to 5d-4f transition of Ce^{3+} ion, their light outputs are insufficient (about 3000 ph/n) (Yanagida et al., 2011b) for use in actual applications.

In this work, Ce-alkali metal (Na, K, Rb and Cs) co-doped LiSAF crystalline scintillators were grown and investigated to understand the effect of co-dopant on scintillation properties. We evaluated (1) the phase structure and chemical composition of the crystals by XRD, (2) the optical properties by absorption spectra and photoluminescence decay time, and finally, (3) the scintillation properties by radioluminescence spectra and pulse height spectra. From these experiments, we determined the suitable co-dopant for Ce doped LiSAF crystalline scintillator.

2. Experiments

Crystal samples with Ce 1 mol% and alkali metal 1 mol% co-doped LiSAF were grown by the Micro-Pulling Down (μ-PD) method with an RF heating system (Yoshikawa et al., 2004). Mixtures of 4N LiF (95% ^{6}LiF), SrF_2, AlF_3, NaF, KF, RbF and CsF powders produced by Stella Chemifa Corporation Co. Ltd. were used in the stoichiometric ratio as starting materials. After the starting powders were put into the carbon crucible, the chamber was evacuated down to 10^{-4} Pa and heated to about 300 °C for baking out for several hours. Then, the atmosphere was changed in the crucible with the high purity Ar + CF_4 gas (= 9:1) and finally, the crucible was heated up to the melting point of the LiSAF. A thin Pt wire was used as the seed crystal and the pulling speed was 5–6 mm/h.

The grown crystals were cut to the plates of 1 mm thickness and then polished to evaluate the optical and scintillation properties. To identify the phase of the grown crystals, powder X-ray diffraction (XRD) was carried out using RINT-2000 (RIGAKU). The X-ray source was CuKα (accelerating voltage: 40 kV, beam current: 40 mA).

Transmittance spectra and reflectivity were measured with spectrophotometer (V-550, JASCO and UV-2550, Shimadzu, respectively) in the 190–900 nm wavelength range. The tungsten lamp (370–900 nm) and the deuterium lamp (190–370 nm) were used as a light source. The results obtained from the spectra were used to calculate the absorption coefficient. To study the luminescence properties of the crystals, photoluminescence decay times were measured by a modified spectrofluorimeter (FLS920 Edinburgh Instruments). A hydrogen nanosecond flashlamp was used for the photoluminescence decay measurements as an excitation source using the method of time-correlated single photon counting. Using the detection part of the same spectrofluorimeter, radioluminescence spectra under ^{241}Am α-ray were measured. The α-ray excitation simulates the ^{6}Li(n, α)^{3}H reaction where charged particles excite the scintillation material with high Q-value of 4.8 MeV. The scintillation light yields were evaluated with Photo Multiplier Tube (PMT, R8778, Hamamatsu) with which they were coupled with an optical grease (Krytox16350, DuPont). The crystals were covered with Teflon tapes and the ^{252}Cf (<3.7 MBq) radioisotope was used as the neutron source. The signals were directly fed into a shaping amplifier (ORTEC 572) and a multichannel analyzer (MCA, Amptek 8000A). The PMT was surrounded by 43 mm thick polyethylene layer serving as the moderator and reflector. In addition, Pb block of 50 mm thickness was set between the crystal and the ^{252}Cf source to reduce gamma-ray background. In the measurements, a Li-glass scintillator GS20 that has light yield of 6000 ph/n (Van Eijk, 2004) was used as a reference sample. At the same time, decay time profiles were also recorded by WE7311 digital oscilloscope (Yokogawa).

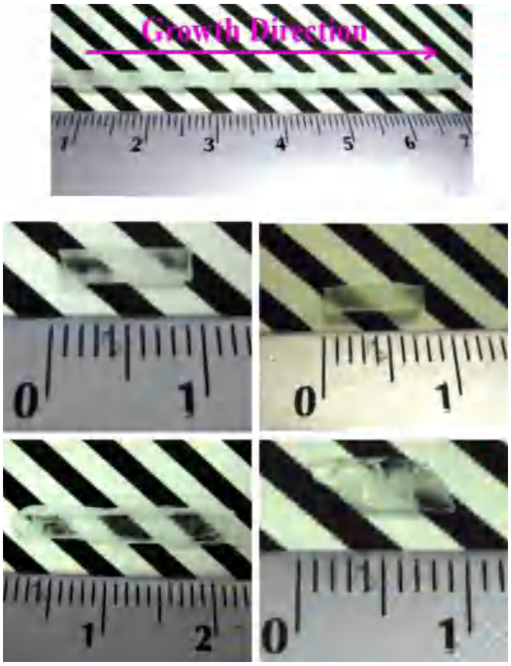

Fig. 1. As grown of Ce–K co-doped LiSAF (top) and polished grown crystals. Clockwise from the top left, Ce–Na, Ce–K, Ce–Cs and Ce–Rb co-doped LiSAF crystals.

3. Result

The crystals of Ce 1% and alkali metal (Na, K, Rb and Cs) 1% co-doped LiSAF were successfully grown by μ-PD as shown in Fig. 1. Despite most of the parts were transparent, some milky parts due to secondary phase were also observed in the crystal. To confirm the phase of the milky parts, the powder XRD patterns of Ce–Na co-doped and non-doped LiSAF crystals were compared in Fig. 2(a). The secondary phase was identified as CeF_3 and then, this is consistent with the results of heavily Ce doped LiSAF (Yamaji et al., 2012). The existence of alkali metal phase or compounds were not detected. Additionally, the lattice constants of the crystals are summarized in Fig. 2(b). According to this result, the a axis slightly decrease compared to non doped one due to dopant, while the c axis decreased.

Taking into account transmittance and reflectivity, the absorption coefficient was calculated using Lambert–Beer law, and the results are shown in Fig. 3. All the crystals showed sharp absorption peaks at 270 nm due to 4f-5d transitions of Ce^{3+} ion. The systematic effect of co-doping on absorption wavelength was not clearly observed. The decay times under 270 nm excitation were determined using a single exponential equation fitting by a deconvolution with instrumental response. Taking into account the instrumental peak, the determined decay times for Ce only, Ce–Na, K, Rb and Cs co-doped crystals were 23, 28, 27, 27 and 24 ns, respectively. Thus, the decay times of the co-doped crystals were comparable or slightly longer than that for the Ce only doped one and these results are consistent with those of Eu-alkali metal co-doped LiSAF.

Then, the radioluminescence spectra of the crystals under ^{241}Am α-ray excitation are shown in Fig. 4. All the crystals showed intense emission band around 280–400 nm and this ultraviolet emission was assigned to the transition from Ce^{3+} 5d state to the 4f ground state levels $^2F_{5/2}$ and $^2F_{7/2}$. The effect of co-doping on the

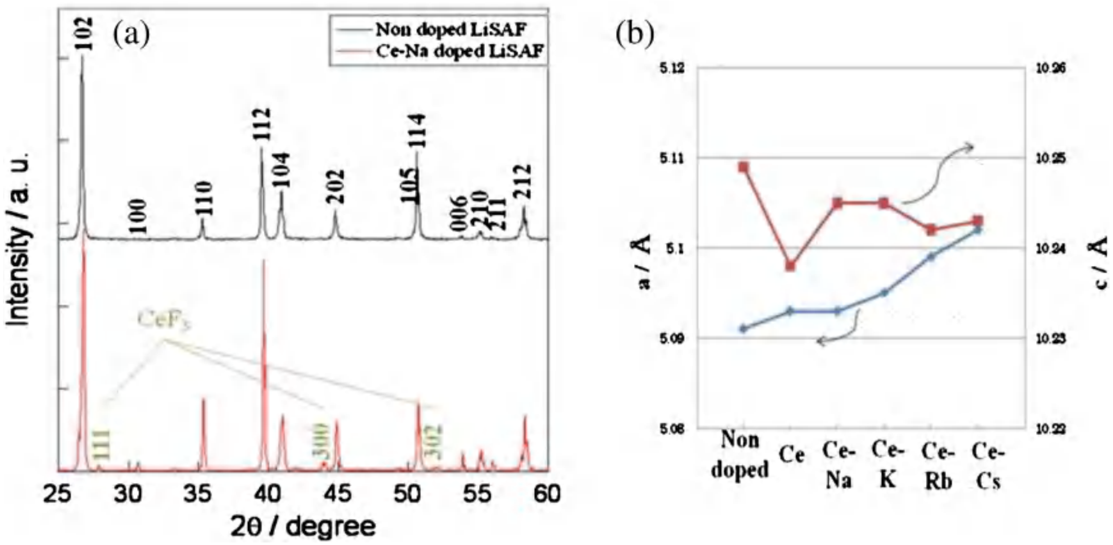

Fig. 2. (a) Powder XRD patterns of non doped and Ce–Na co-doped LiSAF crystals. (b) Lattice parameters of non doped, Ce only, Ce–Na, K, Rb and Cs co-doped LiSAF crystals.

scintillation emission wavelength was also not observed. Furthermore, the luminescence ascribed to CeF_3 phase, which was detected in Powder XRD experiment, was not observed. This wavelength was suitable for the efficiency of R7600 PMT and then, we chose the PMT for the a-ray induced decay kinetics, neutron induced light yield and decay kinetics experiments. The scintillation decay times of the crystals were measured under α-ray excitation using PMT and oscilloscope. The scintillation decay times of Ce only, Ce–Na, K, Rb and Cs co-doped crystals were determined using double exponential equation fitting and the decay times of each fast component were ~59, ~60, ~71, ~68 and ~70 ns, respectively. These fast component ratios were almost 90% and they were attributed to Ce^{3+} 5d-4f transition, while slow components showed decay times of several hundred ns and its origin is unclear. However, the existence of the slow components for example in Ce:LiSAF was also reported in previous studies (Shiran et al., 2005). As in the case of the result of photoluminescence decay times, the leading decay times of the co-doped crystals were slightly longer than that of the Ce only doped. Moreover, the difference between the photoluminescence and scintillation decay times were consistent with the result of Ce:LiCAF (Yanagida et al., 2009). The origin of the delay of scintillation light is connected with the energy transfer from host lattice to luminescence centers.

The thermal-neutron-induced light yields of the crystals were investigated, as shown in Fig. 5. Considering the decay times, the shaping times were set to be 2 μs. The peak channel numbers of GS20, Ce only, Na, K, Rb and Cs co-doped crystals were 474, 155, 332,

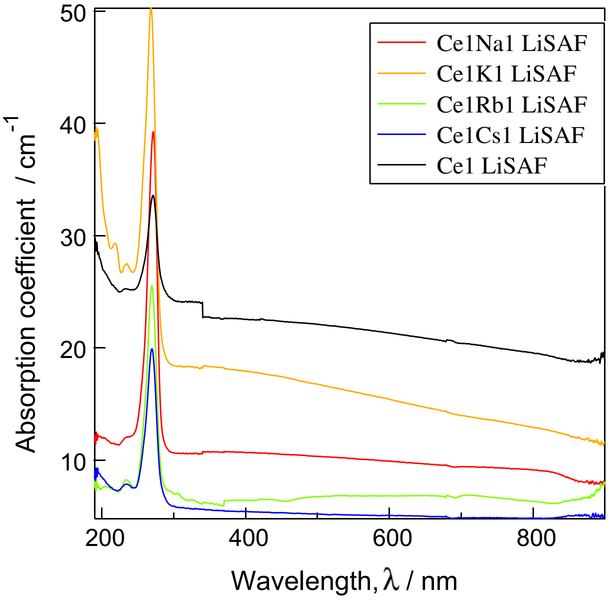

Fig. 3. The absorption spectra of the crystals. Red, orange, green, blue and black curve represent Ce–Na, K, Rb, Cs co-doped and Ce only doped LiSAF, respectively. (For interpretation of the references to colour in this figure legend, the reader is referred to the web version of this article.)

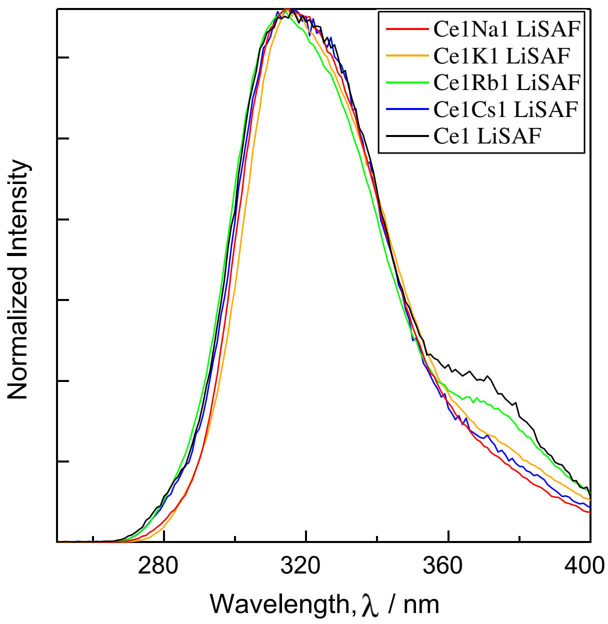

Fig. 4. The radioluminescence spectra of the crystals under ^{241}Am α-ray. Red, orange, green, blue and black curve represent Ce–Na, K, Rb, Cs co-doped and Ce only doped LiSAF, respectively. (For interpretation of the references to colour in this figure legend, the reader is referred to the web version of this article.)

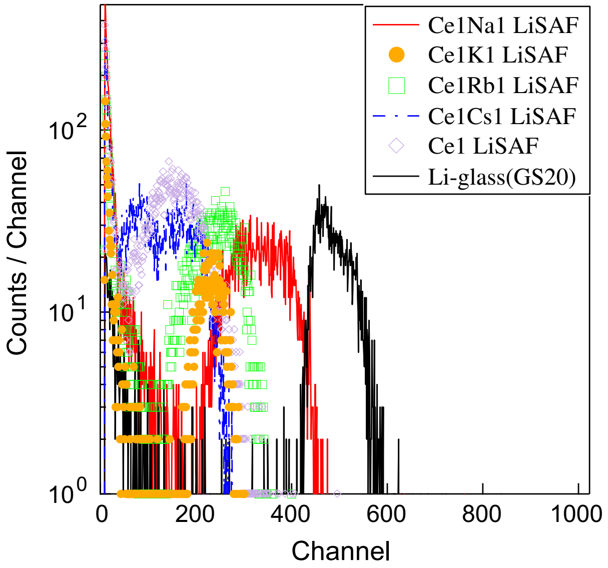

Fig. 5. The pulse height spectra induced by ^{252}Cf thermal neutron. Ce–Na (red curve), K (orange dot), Rb (green square), Cs (blue dot-line) co-doped and Ce only (black curve) doped LiSAFs were displayed, respectively. (For interpretation of the references to colour in this figure legend, the reader is referred to the web version of this article.)

230, 245 and 170, respectively. Thus, the light yields of all the co-doped crystals were improved with respect to the Ce only doped one and calculated to be ~4200, ~2950, ~3100 and 2100 ph/n. Considering the light yield of the Ce only doped to be ~2000 ph/n, the Ce–Na co-doped crystal outperformed the Ce only doped one by approximately 2 times. Thus, in the case of Ce doped LiSAF crystal, Na might be suitable co-dopant for improving the scintillation properties, while K might be the most suitable in the case of Eu doped LiSAF (Wakahara et al., 2012).

At the same time, the scintillation decay times of the crystals under thermal neutron were also measured and the decay curves were well reproduced by single exponential function. The scintillation decay times of Ce only, Ce–Na, K, Rb and Cs co-doped crystals were ~61, ~65, ~67.5, ~67.4 and ~63 ns, respectively. Thus, similarly to the decay result using the other excitation sources, the decay times related to the co-doped samples were slightly longer than that of Ce only doped one. Fig. 6 shows the decay times of the crystals using various excitation sources including 270 nm photons, ^{241}Am α-ray and ^{252}Cf neutron. All the dependences have similar trend, while that the values for the alkali metal co-doped crystals were slightly longer than that of the Ce only doped one. These results are consistent with the previous report about Eu-alkali metal co-doped LiSAF (Wakahara et al., 2012). Generally speaking, the decay time of Ce activated material becomes decreasing with increasing the Ce concentration (Fukabori et al., 2011; Ishibashi et al., 1989). Although we could not estimate the actual Ce segregation coefficient, in the case of this study, it is considered that the alkali metal co-doping might not influence the Ce segregation coefficient. However, the light yields were improved by co-doping, especially the Ce–Na co-doped LiSAF showed the highest light yield. Though the role of Na co-doping was not understood, Na co-doping improves the probability of energy transfer from the host lattice to the Ce^{3+} emission center, while slight prolonging of the decay time can be caused by delayed transport of the charge carriers temporarily trapped on the Na-related trapping levels.

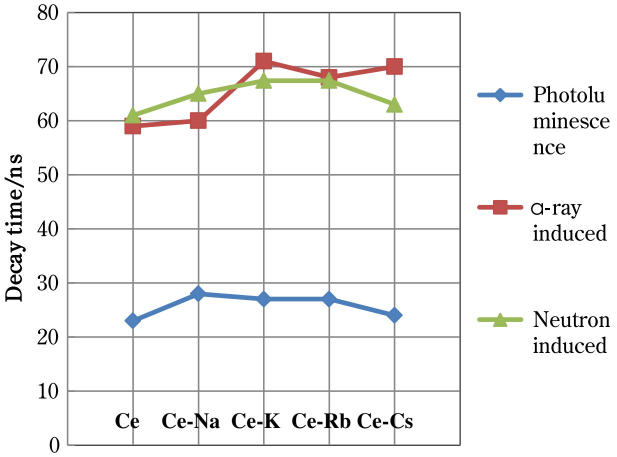

Fig. 6. The decay times of the LiSAF crystals induced by photo (blue), a-ray (red) and neutron (green), respectively. (For interpretation of the references to colour in this figure legend, the reader is referred to the web version of this article.)

4. Conclusion

Ce-alkali metal co-doped LiSAF crystals were successfully grown by μ-PD method to develop the novel scintillation material for thermal neutron detector. In absorption coefficient spectra, all the crystals showed sharp peak ascribed to Ce^{3+} 4f-5d transition at 270 nm. In the radioluminescence of the crystals under ^{241}Am a-ray only the luminescence related to Ce^{3+} 5d-4f transition around 280–400 nm was observed while the emission of CeF_3 was absent. The effect of the alkali metal co-dopants was not observed in absorption and emission wavelength measurements. The decay times under several excitation sources including 270 nm photons, ^{241}Am a-ray and ^{252}Cf thermal neutrons were measured. Regardless the excitation source, the decay times of co-doped crystals were slightly longer than that of the Ce only doped one. These results were consistent with those for Eu-alkali metal co-doped LiSAF. We also consider that the effect of co-dopant might not be change the Ce segregation coefficient. The light yields of the co-doped crystals were improved compared with Ce only doped one. Especially, Ce–Na co-doped LiSAF crystals showed the best light output about 4200 ph/n and outperformed the Ce only doped one by around 2 times. Na might be the most suitable for Ce:LiSAF as co-dopant in terms of the light yield. And then the light yield improvement by co-doping with slight prolongation of the decay times was consistent with the results for the Eu-alkali metal co-doped LiSAF. Therefore, though the scintillation mechanism of the improvement by alkali metal co-doping is not understood, it is expected that Na co-doping improves the probability of energy transfer from the host lattice to the Ce^{3+} emission center by delayed transport of the charge carriers temporarily trapped on the Na-related trapping levels. However, this is a just hypothetical conclusion; therefore, we have to study the scintillation mechanism in detail to confirm this idea.

Acknowledgment

This work was mainly supported by JST Sentan and partially by a Grant in Aid for Young Scientists (B)-15686001, (A)-23686135, and Challenging Exploratory Research-23656584 from the Ministry of Education, Culture, Sports, Science and Technology of the Japanese government (MEXT). Partial assistance from the Yazaki Memorial Foundation for Science and Technology, Japan Science Society, Sumitomo Foundation, and Iketani Science and Technology Foundation are also gratefully acknowledged.

References

Fukabori, A., Yokota, Y., Yanagida, T., Moretti, F., Chani, V., Kawaguchi, N., Kamada, K., Yoshikawa, A., 2011. Nucl. Instrum. Meth. Phys. Res. A 631, 68–72.

Ishibashi, H., Shimizu, K., Susa, K., 1989. IEEE Trans. Nucl. Sci. 36, 170–172.

Kouzes, R.T., Ely, J.H., Erikson, L.E., Kernan, W.J., Lintereur, A.T., Siciliano, E.R., Stephens, D.L., Stromswold, D.C., Van Ginhoven, R.M., Woodring, M.L., 2010. Nucl. Instrum. Meth. Phys. Res. A 623 (3), 1035.

Shiran, N., Gektin, A., Neicheva, S., Weber, M., Derenzo, S., Kirm, M., True, M., Shpinkov, I., Spassky, D., Shimamura, K., Ichinose, N., 2005. Nucl. Instr. Meth. A 537, 291–294.

Van Eijk, C.W.E., 2004. Radiat. Meas. 38, 337.

Wakahara, S., Yanagida, T., Yokota, Y., Yamaji, A., Pejchal, J., Fujimoto, Y., Sugiyama, M., Kurosawa, S., Kawaguchi, N., Fukuda, K., Yoshikawa, A. Phys. Status Solidi C., in press.

Yamaji, A., Yanagida, T., Kawaguchi, N., Fujimoto, Y., Yokota, Y., Watanabe, K., Yamazaki, A., Yoshikawa, A., Pejchal, J., 2011. Nucl. Instr. Meth. A 659, 368–372.

Yamaji, A., Yokota, Y., Yanagida, T., Kawaguchi, N., Futami, Y., Fujimoto, Y., Yoshikawa, A., 2012. J. Cryst. Growth 352, 106–109.

Yanagida, T., Yoshikawa, A., Yokota, Y., Maeo, S., Kawaguchi, N., Ishizu, S., Fukuda, K., Suyama, T., 2009. Opt. Mater. 32, 311–314.

Yanagida, T., Kawaguchi, N., Fujimoto, Y., Fukuda, K., Yokota, Y., Yamazaki, A., Watanabe, K., Pejchal, J., Uritani, A., Iguchi, T., Yoshika, A., 2011a. Opt. Mater. 33, 1243–1247.

Yanagida, T., Kawaguchi, N., Fujimoto, Y., Yokota, Y., Yamazaki, A., Watanabe, K., Kamada, K., Yoshikawa, A., Chani, V., 2011b. Radiat. Meas. 46, 1708–1711.

Yanagida, T., Yamaji, A., Kawaguchi, N., Fujimoto, Y., Fukuda, K., Kurosawa, S., Yamazaki, A., Watanabe, K., Futami, Y., Yokota, Y., Uritani, A., Iguchi, T., Yoshikawa, A., Nikl, M., 2011c. APEX 4, 106401.

Yokota, Y., Fujimoto, Y., Yanagida, T., Takahashi, H., Yonetani, M., Hayashi, K., Park, I., Kawaguchi, N., Fukuda, K., Yamaji, A., Fukazawa, Y., Nikl, M., Yoshikawa, A., 2011. Cryst. Growth Des. 11, 4775–4779.

Yoshikawa, A., Satonaga, T., Kamada, K., Sato, H., Nikl, M., Solovieva, N., Fukuda, T., 2004. J. Cryst. Growth 270, 427.